

Metallicity effects on open cluster dynamics

Jarrold R. Hurley,^{1,2*} Christopher A. Tout,³ Sverre J. Aarseth³ and Onno R. Pols⁴

¹*Centre for Stellar and Planetary Astrophysics, School of Mathematical Sciences, Monash University, Vic. 3800, Australia*

²*Department of Astrophysics, American Museum of Natural History, Central Park West at 79th Street, New York, NY 10024, USA*

³*Institute of Astronomy, Madingley Road, Cambridge CB3 0HA*

⁴*Astronomical Institute, Utrecht University, Postbus 80000, Utrecht 3508 TA, the Netherlands*

Accepted 2004 September 8. Received 2004 June 25; in original form 2004 February 18

ABSTRACT

We take advantage of an N -body code that treats a range of metallicities to investigate the effect of metallicity on the internal dynamics of star clusters. Simulations of a set of large open clusters without primordial binaries are performed. We find that core collapse is postponed in low-metallicity star clusters, compared with Population I clusters, owing to the increased rate of mass loss through stellar evolution suffered at early times. However, earlier core collapse in high-metallicity clusters leads to an increase in the escape of stars from the cluster. We find that by remarkable cancellation of these two effects cluster dissolution times are little affected by changes in metallicity: high-metallicity clusters dissolve first but the difference is less than 10 per cent of the lifetime. We illustrate the behaviour of key structural properties of star clusters for models of different metallicity. We also look at the effect this has on the stellar populations of the clusters and the incidence of binary formation and exchange interactions. While the effect of metallicity on certain gross characteristics of a star cluster is found to be weak, we also find that in many respects metallicity is an important parameter in the evolution of a star cluster and should not be ignored.

Key words: stellar dynamics – methods: N -body simulations – stars: evolution – stars: mass-loss – globular clusters: general – open clusters and associations: general.

1 INTRODUCTION

It has long been recognized that the effects of stellar evolution are of paramount importance in cluster evolution (Angeletti & Giannone 1977; Applegate 1986; Chernoff & Weinberg 1990). Mass loss in stellar winds and supernovae change the cluster mass and therefore alter the tidal boundary of the cluster and ultimately its lifetime. The rate of relaxation is also affected by changing the individual stellar masses with time and this, combined with an expansion of the cluster, acts to change the time-scale for core collapse. One way to alter the stellar evolution history of a stellar system is to change the metallicity of the stars it contains: stars of the same mass and different metallicity have different evolution time-scales and therefore lose mass at different rates.

In our Galaxy, we find star clusters with two sets of metallicities: open clusters of approximately solar metallicity, $Z = 0.02$, and globular clusters, which typically have lower metallicity. Star clusters in the Large Magellanic Clouds (LMCs) cover a range of sizes and metallicity (Mackey & Gilmore 2003), while models of star cluster evolution that have included stellar evolution have generally been restricted to the use of solar metallicity stellar models. Hurley,

Pols & Tout (2000) devised a stellar evolution prescription that can treat metallicity in the range 0.0001 to 0.03 and incorporated this into an existing N -body code (Hurley et al. 2001) to model star cluster dynamics. This means that star cluster models can be constructed for the full range of metallicities indicated by observations, with detailed evolution of the stars taken into account.

In this paper, we look for the first time at the effect of metallicity on the evolution of a star cluster. We discuss the differences in stellar models produced by changes in metallicity that are pertinent to our investigation in Section 2. In Section 3, we describe our simulation method and in Section 4 we justify the N -body models we have chosen to perform. Section 5 contains the results and this is followed by a discussion and summary.

2 METALLICITY AND STELLAR EVOLUTION

Grids of stellar evolution models for a range of stellar masses and metallicities have been presented in the past (e.g. Schaller et al. 1992; Pols et al. 1998; Girardi et al. 2000; VandenBerg et al. 2000; Yi, Kim & Demarque 2003). A general property of these models is that main-sequence (MS) lifetimes decrease with decreasing metallicity for stars with masses less than approximately $9 M_{\odot}$. Furthermore, for any two metallicities, the difference in lifetimes increases as we look at models of decreasing mass: the difference is as much

*E-mail: jarrod.hurley@sci.monash.edu.au (JRH)

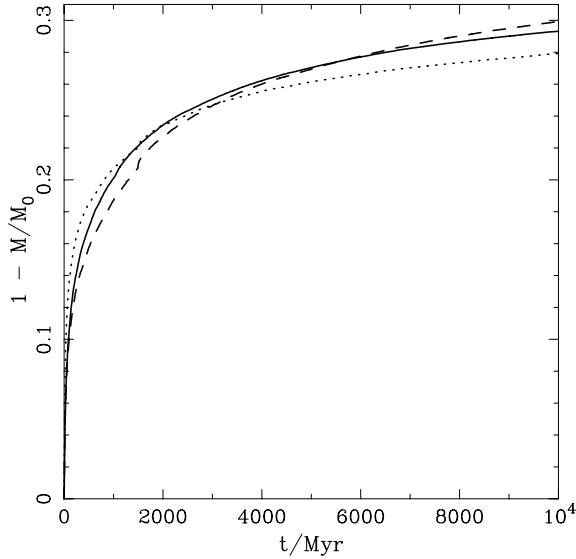


Figure 1. Mass loss owing to stellar evolution arising from various models: Kroupa et al. (1993; KTG) initial mass function (IMF) and $Z = 0.0001$ (solid line), KTG IMF and $Z = 0.02$ (dashed line), and a Salpeter IMF with $\alpha = 2.35$ and $Z = 0.02$ (dotted line). M_0 is the initial total mass and M the total mass at time t .

as 50 per cent between solar-mass models of Population I ($Z = 0.02$) and Population II ($Z = 0.001$) composition. As a result, we would expect a low-metallicity population to have less mass than its high-metallicity counterpart from an age of approximately 40 Myr onwards if comprising the same number of stars drawn from the same initial mass function (IMF). The situation is not so straightforward, however. While it is true that, for substantially evolved populations, a lower metallicity results in a lower MS turn-off mass at a particular age, it cannot be assumed that a star of a particular mass loses the same amount of mass during its lifetime regardless of its composition. The white dwarf (WD) initial–final mass-relation (IFMR) changes with metallicity (e.g. Han, Podsiadlowski & Eggleton 1994; Hurley et al. 2000): for any initial stellar mass the mass of the WD that the star will eventually become is greater for lower metallicity.

To illustrate the mass-loss history of stellar populations with differing metallicity, we take 100 000 stars drawn from the IMF of Kroupa, Tout & Gilmore (1993, KTG) between the limits of 0.1 and $50 M_{\odot}$. We evolve these stars according to the stellar evolution algorithm of Hurley et al. (2000), for $Z = 0.02$ for the whole population and repeat this with $Z = 0.0001$. The results are shown in Fig. 1. We see that the metal-poor population loses mass at a faster rate initially but the situation is reversed from approximately 1.5 Gyr onwards. After 5.5 Gyr, the two populations have lost the same amount of mass although the mass-loss histories to this point have been somewhat different. We note that Hurley et al. (2000) employ the standard Reimers (1975) relation to describe mass loss from giant stars and that no dependence on metallicity is included (see Carraro et al. 1996 for a related discussion). There is a factor $Z^{1/2}$ in the prescription used by Hurley et al. (2000) to model mass loss from massive stars with luminosity in excess of $4000 L_{\odot}$ (see Nieuwenhuijzen & de Jager 1990), but this only acts for the first 30–40 Myr and affects stars of approximately $8 M_{\odot}$ or greater. After 10 Myr, the $Z = 0.02$ population has lost 2.6 per cent of its mass as opposed to 2.2 per cent for the $Z = 0.0001$ population and after 40 Myr both populations have lost 7 per cent of their initial mass.

For comparison, we have evolved an additional $Z = 0.02$ population but this time with the stars drawn from a Salpeter (1955) IMF with slope of $\alpha = 2.35$. The mass limits remain the same as used for the previous populations. Inspection of Fig. 1 raises the possibility that the expected change in evolution of a star cluster when changing the metallicity could be predicted to some extent by comparing models with the same metallicity but with the stars drawn from different IMFs. Comparisons of this type have been performed in the past (e.g. de la Fuente Marcos 1996a) but a crucial distinction is that, by changing the IMF, the total initial mass of the population changes or, if the total mass is constrained to be the same, the number of stars changes. By comparing models with different metallicity for their constituent stars, we have a unique way to explore the effect of mass-loss history on cluster evolution while keeping all other evolution time-scales comparable at the start.

3 SIMULATION METHOD

To model the dynamical evolution of star clusters, we use the NBODY4 code (Aarseth 1999; Hurley et al. 2001). Simulations are performed on GRAPE-6 boards (Makino et al. 2003) located at the American Museum of Natural History.

The KTG IMF is used to distribute the stellar masses, once again with the mass limits of 0.1 and $50 M_{\odot}$. We assume that all stars are on the zero-age main sequence (ZAMS) when the simulation begins and that any residual gas from the star formation process has been removed. Stars are evolved according to the stellar evolution prescription by Hurley et al. (2000), which is based on the detailed models of Pols et al. (1998) and is accurate for a wide range of metallicity.

We use a Plummer density profile (Plummer 1911; Aarseth, Hénon & Wielen 1974) and assume the stars are in virial equilibrium when assigning the initial positions and velocities. Formally the Plummer profile extends to infinite radius, so a cut-off at a radius corresponding to 10 times the half-mass radius is applied in order to deal with rare cases of large distance (Aarseth 2003). We note that when converting from standard scaled N -body units (Heggie & Mathieu 1986) to physical units, a free parameter is the length-scale, R_{sc} , which can be chosen by the NBODY4 user. This converts the N -body unit of length to parsecs and, in combination with the total mass of the cluster, gives the conversion factors to physical units for time and velocity as well.

The cluster is subject to a standard Galactic tidal field (circular orbit at the solar distance) with stars removed from the simulation when their distance from the density centre exceeds twice that of the tidal radius of the cluster. This condition allows for stars on orbits that may momentarily place them exterior to the tidal boundary while remaining bound to the cluster (Giersz & Heggie 1997).

4 CHOICE OF MODEL

There are a number of factors involved in choosing an appropriate number of stars for the initial model. We definitely want N to be large enough that the cluster evolves for at least 6 Gyr before losing all of its stars so that the period of time over which changes in metallicity give a change in mass-loss history but the same net mass loss from stars (approximately 5.5 Gyr) is covered. However, we do not want N to be so large that core collapse occurs much later than this and the time-scale for two-body relaxation and energy equipartition is much greater than the typical stellar evolution time-scale. Such lifetimes are typical of the old open clusters of our Galaxy, such as NGC 188 (Michaud et al. 2004). The escape rate of stars derived by

Hurley et al. (2001) for a cluster subject to the standard Galactic tidal field indicates that a starting model with N in the range of 30 000 to 40 000 stars is appropriate for our needs.

Traditionally an important factor limiting the choice of N when using the direct N -body method is the time taken to complete a simulation. The advent of special-purpose hardware created by the GRAPE project (Makino & Taiji 1998) at Tokyo University to tackle gravitational systems means that for open clusters this is no longer an issue. Baumgardt & Makino (2003) used `NBODY4` on the GRAPE-6 to simulate clusters with as many as 131 072 stars in a timely manner. It was also demonstrated by de la Fuente Marcos & de la Fuente Marcos (2002) that models of open clusters are within the scope of parallel computers. Common to both of these studies is the absence of primordial binaries, which produce a sharp increase in simulation time when present in non-negligible numbers (Makino & Hut 1990). This is even after much effort has been invested to improve the algorithms that treat binary processes (see Aarseth 2003).

We have chosen to start with $N = 30\,000$ and to simplify matters by only including single stars, though the binaries that form during the simulation are evolved in detail by the Hurley, Tout & Pols (2002) prescriptions. Each model of this type takes approximately 4 d to complete on a 32-chip GRAPE-6 board.

Single-star models, while fairly idealized, are a necessary first step in any systematic study to understand the evolution of star clusters and aid comparison with previous studies that have taken the same approach: albeit without the benefit of metallicity as a free parameter. Such studies include Giersz & Heggie (1994), de la Fuente Marcos (1995) and Portegies Zwart et al. (1998). The fact that we have not included primordial binaries means that our results should not be used to interpret observations of binary-rich open clusters (Montgomery, Marschall & Janes 1993). Certainly N -body models with primordial binaries (McMillan, Hut & Makino 1991; Heggie & Aarseth 1992; de la Fuente Marcos 1996b; Portegies Zwart et al. 2001; Hurley & Shara 2003) have confirmed their significant impact on the evolution and characteristics of open clusters. In a future paper, we shall report on work in progress that expands the parameter space of our study to include the dynamical evolution of binary-rich clusters. For this, the single-star models presented here will provide a template for quantifying the effect of the primordial binary population. Alternative density profiles, e.g. King (1966) models, will also be explored. At this point, we have also neglected to study the effects of varying the strength of the tidal field in which our model clusters reside. This has the potential to alter the cluster lifetime drastically and has been the subject of a number of previous N -body studies (Giersz & Heggie 1997;

Vesperini & Heggie 1997; Portegies Zwart et al. 2002; Baumgardt & Makino 2003). For an overview of the N -body method and more generally the art of star cluster simulation, we suggest Heggie & Hut (2002) and Aarseth (2003).

5 RESULTS

We have performed a variety of simulations and these are summarized in Table 1. In addition to treating metallicity as a model variable, we have also looked at models with differing initial mean density by varying R_{sc} . A scale $R_{\text{sc}} = 5.5$ gives a cluster that fills its tidal radius. By this we mean that the outermost star drawn from the density profile sits at the tidal boundary, which for our truncated Plummer model gives a tidal radius approximately 10 times greater than the cluster half-mass radius. To reduce the effect of statistical fluctuations, we repeated each distinct model so that all results presented in this work are averaged over two simulations.

5.1 General evolution trends

A general description of the evolution of a star cluster including a mass spectrum, mass loss from stellar evolution and a tidal field (e.g. de la Fuente Marcos 1996a; Giersz & Heggie 1997) is as follows. Mass lost from the cluster owing to stellar evolution drives an overall expansion. This is an ongoing effect throughout the evolution but is most pronounced during the early stages. The processes of energy equipartition and mass segregation operate from the start and cause the heaviest stars to sink towards the centre while the light stars are heated on a time-scale less than the two-body relaxation time-scale. Low-mass stars escape preferentially from the core and remove kinetic energy, and a density contrast develops, which leads to the gravothermal instability driving what is commonly known as core collapse (Chernoff & Weinberg 1990; Giersz & Heggie 1994; Baumgardt et al. 2003). During core collapse, the inner parts of the cluster flow inwards and, owing to energy conservation, the outer parts move outwards (Meylan & Heggie 1997). However, if the cluster is limited by the tidal field of the Galaxy, the outpouring of energy pushes mass across the tidal boundary and causes it to contract. Eventually the outer regions of the cluster progressively (from the limiting radius inwards) feel the effect of the contracting tidal radius and fall in line in an effort to maintain constant density (Giersz & Heggie 1997).

This behaviour is illustrated in Fig. 2, which shows the evolution of selected Lagrangian radii as well as the core, r_c , and tidal, r_t , radii in model 3 ($Z = 0.02$, $R_{\text{sc}} = 3.0$), which we deem to be our

Table 1. Simulations performed in this work. All models began with $N = 30\,000$ and no binaries. The first column gives an identification number for each model. Next are the metallicity and length-scale. The numbers of stars remaining bound to the cluster after 1, 5 and 9 Gyr of evolution are given in the next three columns. These are followed by the time at which the first binary formed and the time of core collapse. Finally, we show the difference between the core-collapse times found for the two simulations performed of each type. Note that the results in columns 4–8 are averages of the two simulations performed for each distinct model.

#	Z	R_{sc}	N (1 Gyr)	N (5 Gyr)	N (9 Gyr)	$T_{\text{bin}}/\text{Myr}$	T_{cc}/Myr	$\Delta T_{\text{cc}}/\text{Myr}$
1	0.0001	3.0	27796	9930	785	2060	2520	130
2	0.001	3.0	27830	10161	960	1570	2670	150
3	0.02	3.0	27602	8997	385	840	1350	60
4	0.03	3.0	27675	8753	378	510	1760	130
5	0.0001	5.5	26065	11102	1296	4950	6080	240
6	0.001	5.5	26203	11175	1477	5750	5910	370
7	0.02	5.5	26016	9498	590	3910	5350	350
8	0.03	5.5	26122	9515	521	4950	5350	240

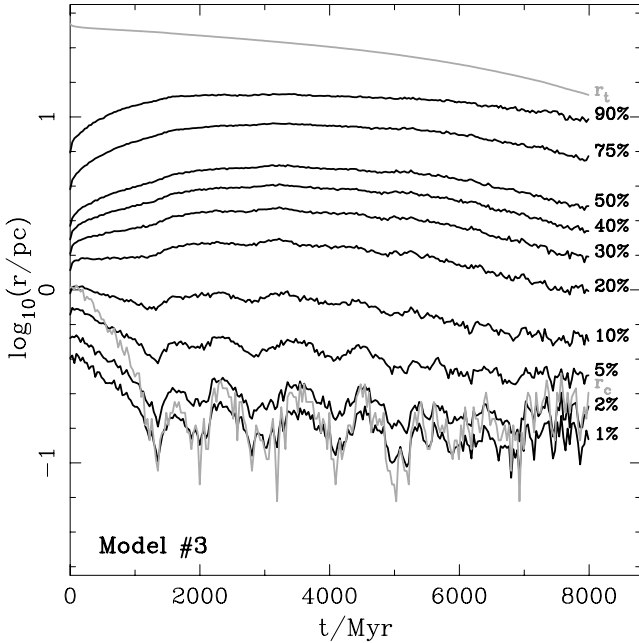


Figure 2. Evolution of selected Lagrangian radii in model 3 ($Z = 0.02$, $R_{sc} = 3.0$). The core and tidal radii are shown as well.

standard model. We only show the evolution up to 8 Gyr. Beyond this time, N drops below 1000 and the behaviour of many key cluster parameters becomes irregular owing to small number statistics. There is an initial expansion of all regions within the cluster, i.e. violent relaxation, as the most massive stars evolve rapidly to become either neutron stars or black holes via supernovae outbursts and a rapid mass loss ensues. This is quickly followed by the onset of core collapse, which leads to contraction from approximately the 20 per cent radius inwards. Outer regions of the cluster continue to expand as a result of stellar evolution driven mass loss, though we note that the length-scale gives a maximum radius initially less than the tidal radius, until the shrinking tidal radius leads to contraction after a few Gyr. We see that core collapse for this model is reached at approximately 1.4 Gyr. By this time two hard binaries (Heggie 1975) have formed. Collapse is followed by a core bounce and subsequent core oscillations (Goodman 1987). Post-collapse expansion is felt at all radii out to the half-mass radius, r_h , and slightly beyond although the effect diminishes with increasing radius. The interested reader can compare the behaviour of our 30 000 star models with that of the $N = 500$ models produced by Giersz & Heggie (1997): in particular their fig. 1 was used as a template for our Fig. 2.

As noted by Chernoff & Weinberg (1990) in analysis of their multimass Fokker–Planck models, the inclusion of stellar evolution, and the associated mass loss, prevents prompt core collapse and also postpones subsequent collapse. It was then shown by de la Fuente Marcos & de la Fuente Marcos (2002) using N -body models of 10 000 stars that the postponement of core collapse, in conjunction with restricted binary formation, means that stellar evolution actually extends open cluster lifetimes. Conversely, it could be expected that the combined effects of mass loss and expansion would lead to shorter dissolution times for clusters subject to a tidal field. This was found by Portegies Zwart et al. (2001), though the result of these competing effects may depend somewhat on the cluster size (Portegies Zwart et al. 1998) and the time-scales involved

(Aarseth & Heggie 1998), but they are definitely of interest in regard to understanding the evolution of clusters of different metallicity.

5.2 Effect of cluster mean density

The primary goal of this work is to explore the effect that metallicity has on cluster evolution by changing the stellar evolution time-scale. Bearing in mind that mass loss from stellar evolution drives an expansion of a star cluster and that previous work has shown that the initial structure of a cluster affects the core collapse and disruption time-scales (Baumgardt & Makino 2003, and references within), we feel it is important to take a qualitative look at how the evolution changes when we vary the initial concentration before we proceed to consider metallicity as a parameter. We do this simply by increasing the length-scale used in our standard model (model 3: $Z = 0.02$, $R_{sc} = 3.0$) to a value that gives a cluster filling its tidal radius from the start (model 7: $Z = 0.02$, $R_{sc} = 5.5$). This means that both r_c and r_h increase while their ratio remains the same. To avoid inferring that we are looking at models of different central concentration, in which the ratio of r_c to r_h varies, we will talk in terms of varying the mean density of our starting models as opposed to the concentration of the stars. We note that the cluster crossing time is proportional to $R^{3/2}$, where R is the cluster radius, so that a change to R_{sc} alters the dynamical time-scale of the model.

Fig. 3 shows the evolution of selected radii in model 7 and should be compared directly with Fig. 2. We compare the evolution of the cluster mass and the mass lost in escaping stars for models 3 and 7 in Fig. 4. The main points to note are that lower mean-density results in more mass lost in escaping stars and delayed core collapse. This is as expected. However, the shorter relaxation time of the more condensed model, and associated earlier core collapse, accelerates the escape of stars and means that overall the two models have similar dissolution times.

In Fig. 5, we highlight the evolution of the key quantities r_c and r_h . The velocity dispersion, σ_{disp} , of the two models is compared in Fig. 6 and the average stellar mass, m_{av} is compared in Fig. 7. At the start, r_c and r_h are bigger and σ_{disp} smaller in model 7, as

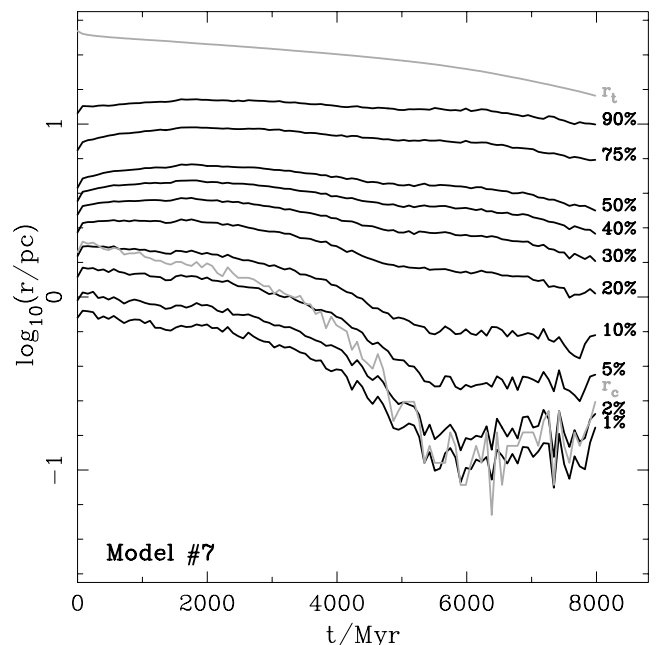


Figure 3. As Fig. 2 but for model 7 ($Z = 0.02$, $R_{sc} = 5.5$).

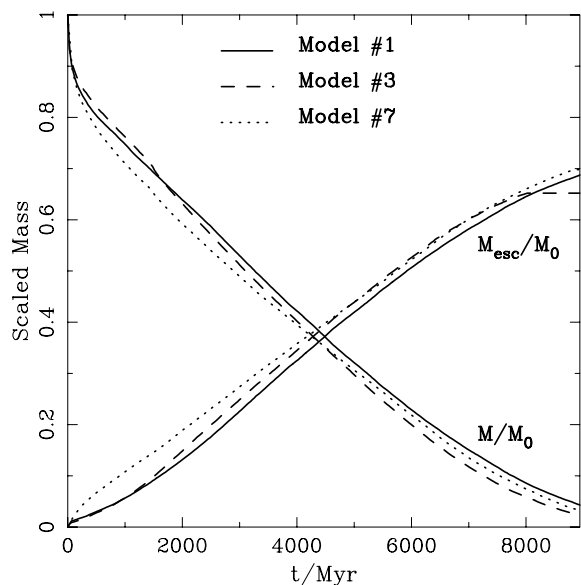


Figure 4. Evolution of the mass remaining in the cluster (lines starting from a scaled mass of 1 at 0 Myr) and the mass lost in escaping stars (lines starting from a scaled mass of 0) in models 1 (solid lines: $Z = 0.0001$, $R_{\text{sc}} = 3.0$), 3 (dashed lines: $Z = 0.02$, $R_{\text{sc}} = 3.0$) and 7 (dotted lines: $Z = 0.02$, $R_{\text{sc}} = 5.5$). Note that masses are scaled by the initial cluster mass.

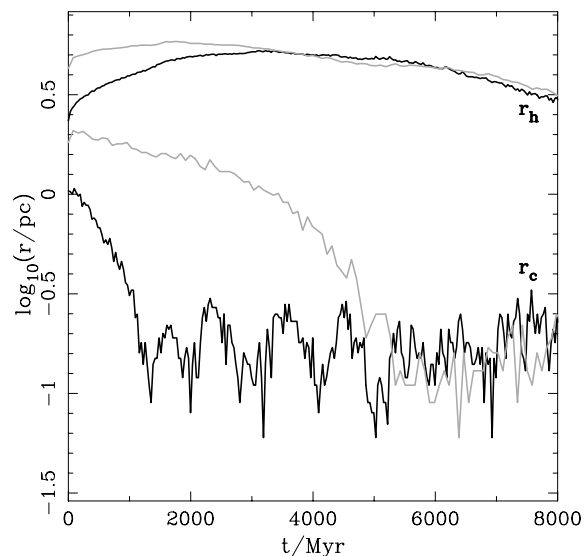


Figure 5. Comparison of the evolution of the core radius and half-mass radius for models 3 (solid dark lines: $Z = 0.02$, $R_{\text{sc}} = 3.0$) and 7 (solid grey lines: $Z = 0.02$, $R_{\text{sc}} = 5.5$). Note that for each model the core radius is always interior to the half-mass radius.

expected. Now a lower mean density means that initially more stars reside near the tidal boundary so that the cluster is more susceptible to losing stars during stellar evolution driven cluster expansion (see Fig. 4). Outer regions of the cluster still expand during the early mass-loss stage (see Fig. 3) but not by as large a factor as we see in model 3 and the duration of the expansion phase is shorter because the effect of the shrinking tidal radius is felt much earlier. Compare the behaviour of r_h in Fig. 5. We also see that the less condensed model takes longer to reach core collapse. This is partly because r_c is larger to begin with but the overriding factor is that it takes

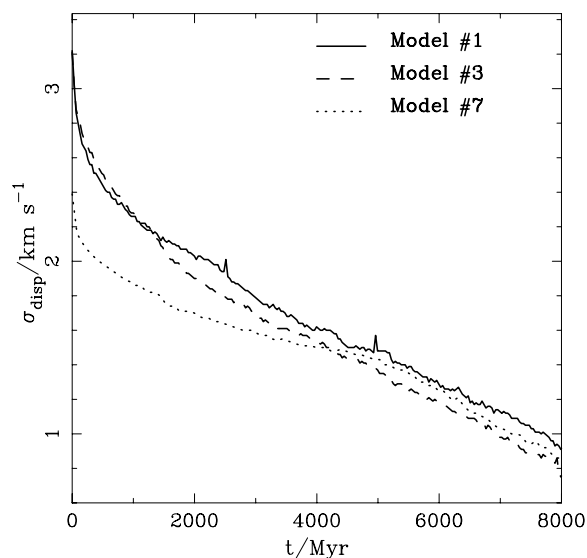


Figure 6. Comparison of the evolution of the velocity dispersion for models 3 (dashed line: $Z = 0.02$, $R_{\text{sc}} = 3.0$) and 7 (dotted line: $Z = 0.02$, $R_{\text{sc}} = 5.5$). The velocity dispersion for model 1 (solid line: $Z = 0.0001$, $R_{\text{sc}} = 3.0$) is also shown.

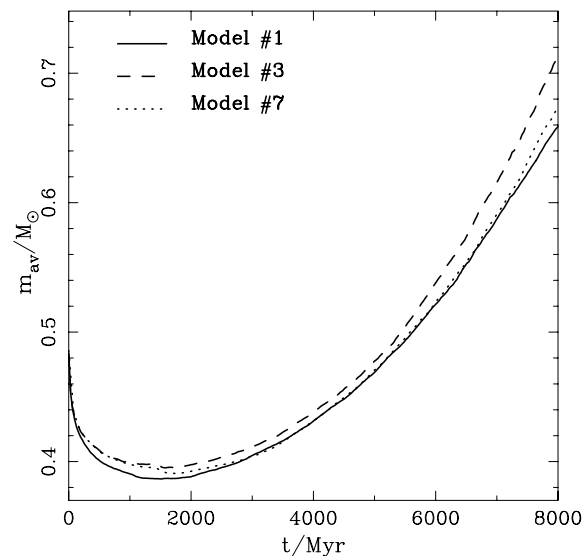


Figure 7. Comparison of the evolution of the average mass of stars in the cluster for models 3 (dashed line: $Z = 0.02$, $R_{\text{sc}} = 3.0$) and 7 (dotted line: $Z = 0.02$, $R_{\text{sc}} = 5.5$). The result for model 1 (solid line: $Z = 0.0001$, $R_{\text{sc}} = 3.0$) is also shown.

longer to develop a significant density contrast. We see this clearly in Figs 2, 3 and 5 where both models evolve to similarly high central densities (reflected in the size of the core and inner Lagrangian radii and also true of the number density) but much earlier in model 3 than model 7, approximately 1.4 Gyr compared with 5.4 Gyr.

Earlier core collapse in model 3, and associated earlier binary presence in the core (see Table 1), acts to increase the rate of escaping stars from the cluster. Eventually the two models reach a point, at approximately 4.3 Gyr, when they have lost the same amount of mass and from then onwards the rate of escape from models 3 and 7 is similar (see Fig. 4). In fact, after approximately 5 Gyr, the characteristics of the two model clusters are remarkably similar

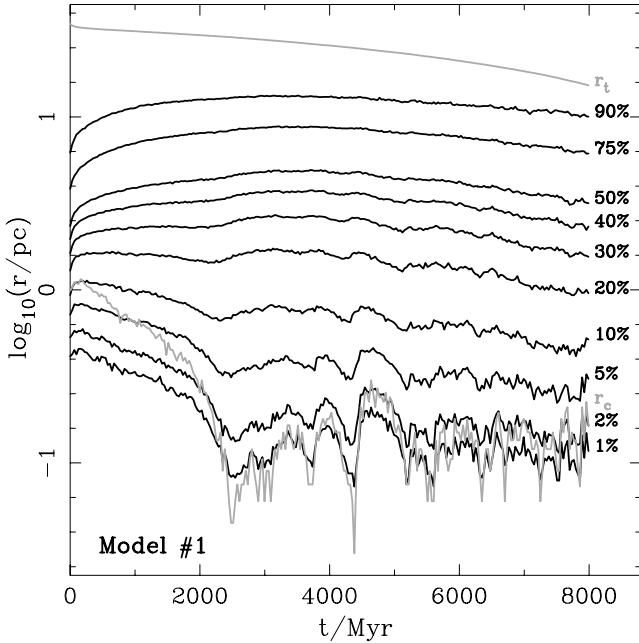


Figure 8. As Fig. 2 but for model 1 ($Z = 0.0001$, $R_{sc} = 3.0$).

for all parameters except for m_{av} . The divergence of m_{av} , lower in model 7 than model 3, reflects the fact that energy equipartition (and therefore mass segregation) develops at a slower rate and that this, combined with the weaker potential well, makes it easier for massive stars to escape in model 7.

5.3 Effect of metallicity

We are now free to focus on our goal of investigating the effect of metallicity on cluster evolution. To this end, we compare our standard model of solar metallicity (model 3: $Z = 0.02$, $R_{sc} = 3.0$) with a model of the same initial mean density but with a much lower metallicity, sub-Population II, for its constituent stars (model 1: $Z = 0.0001$, $R_{sc} = 3.0$). The evolution of cluster mass, velocity dispersion and average stellar mass for model 1 are included in Figs 4, 6 and 7 respectively. Fig. 8 follows the behaviour of the Lagrangian radii in model 1 and Fig. 9 contrasts the evolution of r_c and r_h for models 1 and 3, much as in the previous section for models 3 and 7.

We showed earlier (Section 2) that a population of low-metallicity stars suffers greater mass loss through stellar evolution for the first 5 Gyr or so of evolution. The difference is greatest after approximately 1.5 Gyr. As a result, the low- Z cluster has a smaller mass at early times (the escape rate of the two models is similar; Fig. 4) and expands more, even in the core (Fig. 9). For the period over which all regions of the cluster experience expansion, i.e. approximately the first 100 Myr, the inner 1 per cent Lagrangian radius has 20 per cent more growth in model 1 than model 3. The velocity dispersion is lower, also as a result of the increased expansion, but the difference here is not significant especially when compared with the effect of changing the initial mean density (Fig. 6). We see in Fig. 7 that the average stellar mass is lower for the low- Z cluster. This is partly because shorter MS lifetimes ensure that the MS turn-off mass, M_{TO} , is always lower for low- Z but also because expansion delays energy equipartition and the combined effect allows higher mass stars to escape from the cluster.

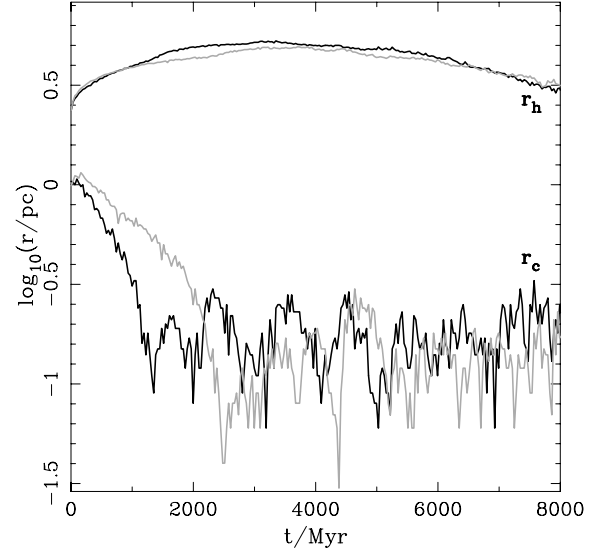


Figure 9. As Fig. 5 but for models 1 (solid grey lines: $Z = 0.0001$, $R_{sc} = 3.0$) and 3 (solid dark lines: $Z = 0.02$, $R_{sc} = 3.0$).

An important difference between the models is that increased expansion and a decreased heavy component act to delay core collapse in low- Z clusters. Chernoff & Weinberg (1990) showed that models with a component of heavier particles, which eventually dominate the central density, and a wider range of stellar masses have shorter diffusion time-scales and so collapse faster. In our case, the higher M_{TO} in model 3 ensures that it has a heavier mass component and wider mass spectrum than model 1, which drives core collapse faster. Compare Figs 2 and 8, which indicate the evolution of density contrast within the two models. The onset of core collapse, earlier in the high- Z cluster, causes expansion of the outer regions (including r_h), earlier binary formation, an increased rate of escape and a lowering of the velocity dispersion. This also means that shortly after it has experienced core collapse the high- Z cluster has become the less massive. So, contrary to initial expectations, it is the high- Z cluster that we expect to dissolve first. This is indeed what we find. Model 3 has been reduced to only 1000 stars after 8180 Myr, while it takes model 1 8780 Myr to reach the same membership. The difference is not substantial, representing a 7 per cent change in the lifetime. However, it shows that the postponement of core collapse and binary formation in model 1, which has the greater stellar evolution mass loss prior to core collapse, extends the cluster lifetime analogous to what was found by de la Fuente Marcos & de la Fuente Marcos (2002) upon the inclusion of stellar evolution in their models.

After both models 1 and 3 have experienced core collapse, the subsequent evolution of r_c and r_h is similar but σ_{disp} (lower in high- Z by approximately 10 per cent) and m_{av} (higher in high- Z by 5–8 per cent) remain distinct. The number density of stars in the core of each model is similar after both have evolved past core collapse, while the number density of stars within r_h is noticeably lower in the high- Z cluster (by as much as a factor of 10).

The time of core collapse and the formation of the first binary are given for all our models in Table 1 along with the cluster membership at chosen times. Comparing models of lower mean density (e.g. models 5 and 7) we find that the metallicity trends are similar but changes occur on longer time-scales. This we would expect from the results of the previous section. Core collapse still occurs earlier in the high-metallicity case with a difference of 730 Myr between models 5 and 7 as opposed to 1170 Myr for the more condensed

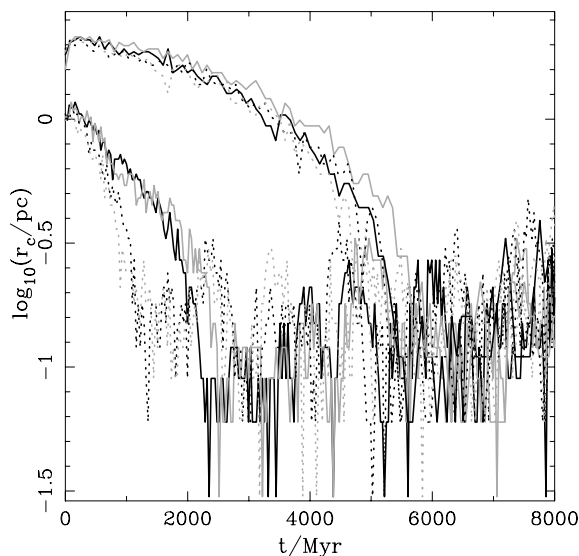


Figure 10. Core radius evolution in all models. Metallicities used in our simulations were: $Z = 0.0001$ (solid dark lines: lower is model 1 and upper is model 5), $Z = 0.001$ (solid grey lines: lower is model 2 and upper is model 6), $Z = 0.02$ (dotted dark lines: lower is model 3 and upper is model 7) and $Z = 0.03$ (dotted grey lines: lower is model 4 and upper is model 8). Note that the evolution for each model is not averaged over the two simulations performed of each type. Instead the results shown are for the first simulation performed for each model.

models 1 and 3. When comparing models 1 and 3, we find that cross-over in the total cluster mass (model 3 becomes less massive) occurs at 1.8 Gyr, while model 3 has the larger half-mass radius from 1.0 Gyr onwards and the lower velocity dispersion after 1.4 Gyr. Inspection of models 5 and 7 shows that the cross-over times for cluster mass, half-mass radius and velocity dispersion are 1.9, 1.5 and 2.0 Gyr, respectively. Once again, it is the high- Z cluster that actually has the shorter dissolution time: model 7 reaches a membership of 1000 stars 800 Myr before model 5.

We have also evolved models with metallicities of $Z = 0.001$ (models 2 and 6) and $Z = 0.03$ (models 4 and 8) for both values of the length-scale parameter. In Fig. 10, we compare the evolution of core radius in models 1–8 but only for the first simulation performed of each model, i.e. the behaviour in this instance is not the average of two simulations. This is repeated in Fig. 11 for the second simulation performed of each model. We see from both these figures that the behaviour of the clusters with $Z = 0.0001$ and $Z = 0.001$ is very similar and that the clusters with $Z = 0.02$ and $Z = 0.03$ also show very similar behaviour to each other. This is also true for all the other parameters we have looked at. In fact, the appearance of the $Z = 0.0001$, 0.001 and $Z = 0.02$, 0.03 models as distinct evolution pairs is even more striking when we look at parameters other than the core radius, which is an intrinsically erratic quantity. This pairing is to be expected because the difference in stellar evolution time-scales is far greater between $Z = 0.001$ and $Z = 0.02$ than it is between $Z = 0.0001$ and $Z = 0.001$ or $Z = 0.02$ and $Z = 0.03$. We also note that differences in evolution owing to a change in metallicity are not as stark for the low-mean density models (see in particular Fig. 10).

Comparison of Figs 10 and 11 gives some idea of the intramodel variations for our N -body simulations. We also show in Table 1 the difference in core-collapse times found for the first and second simulation performed for each model. The procedure of averaging

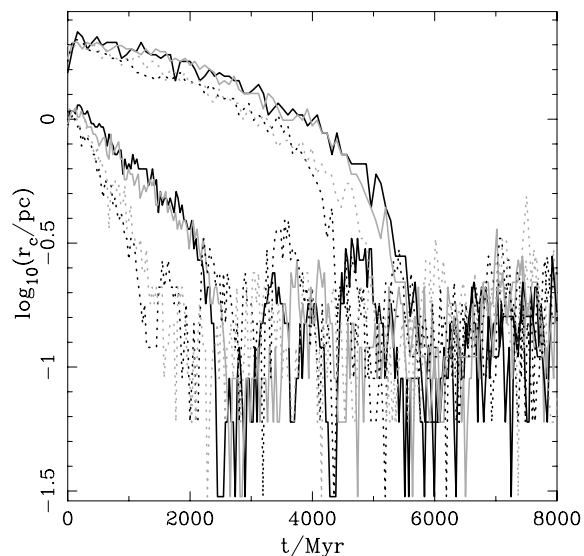


Figure 11. As Fig. 10 but showing the results for the second simulation performed for each model.

Table 2. Stellar data for selected simulations. Note that in this case each row represents the combined results of the two models of that type performed, i.e. numbers are per 60 000 initial stars. The first column gives the identification number for the simulations. The second and third columns give the total number of blue stragglers (BSs) formed and the number of BSs in binary systems. This is followed by the total number of double-white dwarf (WD) binaries, the number of these that have a period less than 1 d and the number of double-WD binaries involved in an exchange interaction. The final column gives the total number of exchange interactions. Only simulation data for the first 8 Gyr of evolution have been considered.

No.	Blue stragglers		Double white dwarfs			Total Exchanges
	Total	Binary	Total	$P < 1$ d	Exchange	
1	13	6	105	10	85	233
3	23	14	10	5	8	242
5	1	0	42	0	38	78
7	4	2	9	4	3	84

the results of N -body simulations is a common practice (e.g. Giersz & Heggie 1997) employed to reduce statistical errors (Smith 1977). This helps to confirm that evolution trends observed in the models are in fact real. We are confident this is the case here as well.

Table 2 lists stellar data for models 1, 3, 5 and 7 in terms of the total number of certain species and events that occurred during the first 8 Gyr of evolution. Certain trends are apparent from Table 2. The first of these is that the number of binary exchange interactions is much larger in the models with higher initial mean density (models 1 and 3). These models experienced core collapse earlier and so have had a longer phase of evolution at high core density. Fig. 12(a) highlights the correlation between the onset of core collapse and the incidence of exchanges. Comparison with Figs 2, 3 and 8 shows the link with central concentration.

It can be seen that the low-metallicity clusters produce a greater number of double-WD binaries. This can be understood in terms of the shorter MS lifetimes and greater core masses for low-metallicity stars, which mean that, at any particular age, a cluster of low Z has more WDs and a greater average WD mass than that of a high- Z cluster. A similar argument explains the greater number of blue

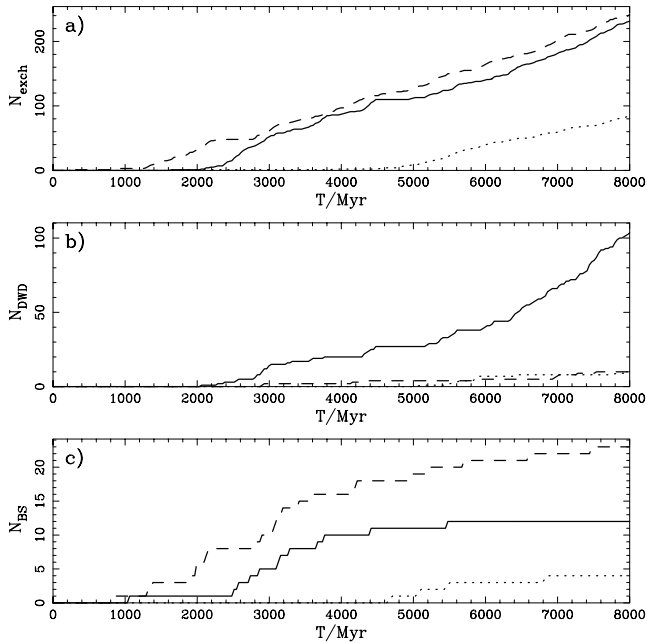


Figure 12. Cumulative number of exchange interactions (top panel), double white dwarfs (WDs; middle panel) and blue stragglers (BSs; bottom panel) in models 1 (solid line: $Z = 0.0001$, $R_{sc} = 3.0$), 3 (dashed line: $Z = 0.02$, $R_{sc} = 3.0$) and 7 (dotted line: $Z = 0.02$, $R_{sc} = 5.5$).

stragglers (BSs) in the high- Z clusters: a greater MS turn-off mass makes it more likely that an MS star will be involved in an exchange interaction and more likely that this MS star would be retained in the emerging binary. In the absence of primordial binaries, collisions between MS stars in eccentric binaries formed from exchange interactions are the main channel for BS formation in an open cluster simulation. Figs 12(b) and (c) show the cumulative number of double-WD binaries and BSs formed in models 1, 3 and 7. We note that a large fraction of the double-WD systems are formed when a WD is exchanged into an existing double WD, with the mass of the interloping WD greater than that of at least one of the original members.

6 DISCUSSION

It has been shown previously that changing the IMF or initial structure of a star cluster can affect its lifetime significantly (e.g. Chernoff & Weinberg 1990; de la Fuente Marcos 1996a; Baumgardt & Makino 2003). In the case of the IMF, a flatter distribution leads to a greater fraction of massive stars, increased mass loss during any violent relaxation phase and an enhanced likelihood of early dissolution. The rapid expulsion of gas from the core of a young cluster may even lead to disruption before the formation process is complete (Vine & Bonnell 2003). The effect of concentration on the dissolution time-scale is not so clear and there may be a dependence on cluster size (Baumgardt & Makino 2003). We note that an accurate description of cluster lifetimes is important for understanding the existence of old open star clusters (Salaris, Weiss & Percival 2004) and the globular cluster mass function (Fall & Zhang 2001; Vesperini & Zepf 2003).

We would expect that the greater rate of mass loss seen in our low-mean density and low-metallicity models for the first few Gyr of evolution would indeed make dissolution more likely in the case of small- N clusters (of the order of a few thousand stars or less),

which have relatively weak potential wells to begin with. For larger N , we have shown that the dissolution time-scale is not significantly affected by varying the initial mean density of the cluster or the metallicity of its stars. However, we have presented a fairly idealized evolution scenario and if other perturbations to the cluster potential exist and are important on a time-scale of a few Gyr or less, then metallicity and initial density become factors that determine the dissolution time-scale. Such perturbations and scenarios that we have neglected may include disc shocking (Vesperini & Heggie 1997), time-varying tidal fields (Baumgardt & Makino 2003; Wilkinson et al. 2003), residence near the Galactic centre (McMillan & Portegies Zwart 2003) and encounters with molecular clouds (Terlevich 1987).

Another important ingredient missing from our models is a primordial binary population. This was omitted quite intentionally so that the effects of varying metallicity would be clear and not masked by a large binary population. There is also no indication how metallicity affects the initial binary distribution. Binaries do form in each of our single star simulations but only in small numbers. As core collapse proceeds and the core density increases, the formation of binaries by dynamical means becomes more likely and is also necessary to avert complete collapse. Typically, 2–3 binaries are present in the core when core collapse comes to a halt and the maximum number of binaries present at any one time is 13 in model 2 at 3.5 Gyr. These binaries play a role in the subsequent evolution of the cluster but the effect is nowhere near as noticeable as that of a large primordial binary population. Hurley & Shara (2003) showed that a primordial binary population of 40 per cent can double the escape rate of stars and reduce the relaxation time-scale. A significant primordial binary population therefore affects the dissolution time-scale and also makes core collapse less pronounced. The evolution of binary-rich open clusters will be the focus of a future paper.

Metallicity has an effect on the appearance of the colour-magnitude diagram (CMD) of a star cluster. However, our models, with relatively low core density and no primordial binaries, do not deviate much from the differences in stellar evolution isochrones of varying metallicity so we have not dwelt on this aspect. That said, binaries do form at different times for our various models and this can lead to fluctuations in the CMD. The escape of stars will also modify the appearance in comparison with standard isochrones. Metallicity differences are more important for globular clusters, e.g. horizontal branch morphology, and the capability to perform N -body models of any metallicity is vital for understanding the internal dynamics and CMDs of these objects.

7 SUMMARY

We have performed a series of model calculations of 30 000 single stars using the state-of-the-art NBODY4 code and treating metallicity and initial mean density as model variables. Stellar evolution is included in the models by taking advantage of a prescription that covers a wide range of metallicity. Binary evolution and the presence of the Galactic tidal field are also accounted for in the N -body simulations. Our 30 000 star models evolve for approximately 10 Gyr before complete dissolution with each simulation requiring 3–4 d of dedicated GRAPE-6 time.

Our standard model with Population I metallicity reaches core collapse after 1.4 Gyr of evolution. We witness the expected behaviour of mass loss from stellar evolution causing an overall expansion of the cluster. This postpones core collapse. The onset of core collapse leads to contraction of the inner regions of the cluster while the outer regions continue to expand. The tidal radius shrinks

in response to mass loss in gas and stars and this causes contraction of the outer regions of the cluster after a few Gyr.

The effect of lowering the initial mean density of the model cluster is that more mass is lost in escaping stars and core collapse is delayed. We find that the dissolution time-scale for a large open cluster is not overly affected by the change in initial mean density because earlier collapse in the more condensed model is accompanied by an increase in the escape rate of stars that counteracts the effect of the weaker potential well of the less condensed model. After the low-mean density model has experienced core collapse at 5.4 Gyr, the subsequent evolution of the models is remarkably similar in terms of observational quantities such as total cluster mass, core radius, half-mass radius, density and velocity dispersion.

Comparing cluster models with different metallicity stars offers an opportunity to explore the effect of mass-loss history on cluster evolution while keeping other time-scales, such as the initial half-mass relaxation time, comparable. Low-metallicity stars have shorter MS lifetimes than their high-metallicity counterparts of the same mass. This means that at any particular age a Population II cluster has a smaller MS turn-off mass than a Population I cluster. However, low-metallicity stars produce more massive WDs. Using the Hurley et al. (2000) evolution algorithm, we find that a population of low-metallicity stars ($Z = 0.001$ or lower) suffers greater mass loss through stellar evolution than a high-metallicity population ($Z = 0.02$ or higher). The difference is greatest at an age of 1.5 Gyr and after 5.5 Gyr the situation is reversed.

We find that the greater mass loss experienced by a low-metallicity cluster during its early evolution leads to an increased expansion of the inner regions of the cluster, as well as a lower velocity dispersion and lower density at the half-mass radius. Core collapse is delayed and occurs at 2.5 Gyr. The earlier core collapse in a high-metallicity cluster produces an expansion of the outer regions of the cluster and earlier binary formation. These effects combine to increase the rate of escape from the cluster and so the high-metallicity cluster is the one with the smaller mass from approximately 1.8 Gyr onwards. In fact, it is the high-metallicity cluster that dissolves first by approximately 700 Myr: a difference of just less than 10 per cent in overall lifetimes. Differences in evolution owing to a change in metallicity are less pronounced in low-mean density models.

The onset of binary formation by dynamical means is directly linked to the time of core collapse and the associated higher stellar density this produces. Exchange interactions require binary formation before becoming a factor and as such their incidence is also linked to core collapse. The number of exchange interactions is much less in the low-mean density models. High-metallicity clusters form more BSs while low-metallicity clusters have a greater number of double-WD binaries. A high proportion of the latter are formed from exchange interactions involving existing double-WD binaries.

We have shown that metallicity is an important parameter that cannot be ignored in simulations of star cluster evolution. Not only does it alter the appearance of the cluster CMD but it also affects the time-scales for core collapse and dissolution, the structural properties of the cluster and the nature of the stellar populations. The use of Population I stellar evolution models in globular cluster simulations may therefore give misleading results.

ACKNOWLEDGMENTS

This work was partially supported by NASA through Hubble Fellowship grant HST-HF-01149.01-A awarded to JRH by the Space Telescope Science Institute, which is operated by the Association

of Universities for Research in Astronomy, Inc., for NASA, under contract NAS 5-26555. CAT thanks Churchill College for a Fellowship. We acknowledge the generous support of the Cordelia Corporation and that of Edward Norton, which has enabled the American Museum of Natural History (AMNH) to purchase new GRAPE-6 boards and supporting hardware. Special thanks goes to John Ouellette for his tireless efforts in setting up and maintaining the AMNH GRAPE-6 boards.

REFERENCES

- Aarseth S. J., 1999, *PASP*, 111, 1333
Aarseth S. J., 2003, *Gravitational N-body Simulations: Tools and Algorithms*. Cambridge Univ. Press, Cambridge
Aarseth S. J., Heggie D. C., 1998, *MNRAS*, 297, 794
Aarseth S., Hénon M., Wielen R., 1974, *A&A*, 37, 183
Angeletti L., Giannone P., 1977, *A&A*, 58, 363
Applegate J. H., 1986, *ApJ*, 301, 132
Baumgardt H., Makino J., 2003, *MNRAS*, 340, 227
Baumgardt H., Heggie D. C., Hut P., Makino J., 2003, *MNRAS*, 341, 247
Carraro G., Girardi L., Bressan A., Chiosi C., 1996, *A&A*, 305, 849
Chernoff D. F., Weinberg M. D., 1990, *ApJ*, 351, 121
Fall S. M., Zhang Q., 2001, *ApJ*, 561, 751
de la Fuente Marcos R., 1995, *A&A*, 301, 407
de la Fuente Marcos R., 1996a, *A&A*, 308, 141
de la Fuente Marcos R., 1996b, *A&A*, 314, 453
de la Fuente Marcos R., de la Fuente Marcos C., 2002, *Ap&SS*, 280, 381
Giersz M., Heggie D. C., 1994, *MNRAS*, 268, 257
Giersz M., Heggie D. C., 1997, *MNRAS*, 286, 709
Girardi L., Bressan A., Bertelli G., Chiosi C., 2000, *A&AS*, 141, 371
Goodman J., 1987, *ApJ*, 313, 576
Han Z., Podsiadlowski Ph., Eggleton P. P., 1994, *MNRAS*, 270, 121
Heggie D. C., 1975, *MNRAS*, 173, 729
Heggie D. C., Aarseth S. J., 1992, *MNRAS*, 257, 513
Heggie D. C., Hut P., 2002, *The Gravitational Million-Body Problem*. Cambridge Univ. Press, Cambridge
Heggie D. C., Mathieu R. D., 1986, in Hut P., McMillan S., eds, *Lecture Notes in Physics 267, The Use of Supercomputers in Stellar Dynamics*. Springer-Verlag, Berlin, p. 233
Hurley J. R., Shara M. M., 2003, *ApJ*, 589, 179
Hurley J. R., Pols O. R., Tout C. A., 2000, *MNRAS*, 315, 543
Hurley J. R., Tout C. A., Aarseth S. J., Pols O. R., 2001, *MNRAS*, 323, 630
Hurley J. R., Tout C. A., Pols O. R., 2002, *MNRAS*, 329, 897
King I. R., 1966, *AJ*, 71, 64
Kroupa P., Tout C. A., Gilmore G., 1993, *MNRAS*, 262, 545 (KTG)
Mackey A. D., Gilmore G. F., 2003, *MNRAS*, 338, 85
McMillan S. L. W., Portegies Zwart S. F., 2003, *ApJ*, 596, 314
McMillan S. L. W., Hut P., Makino J., 1991, *ApJ*, 372, 111
Makino J., Hut P., 1990, *ApJ*, 365, 208
Makino J., Taiji M., 1998, *Scientific Simulations with Special-Purpose Computers: The GRAPE Systems*. John Wiley & Sons, Chichester
Makino J., Fukushige T., Koga M., Namura K., 2003, *PASJ*, 55, 1163
Meylan G., Heggie D., 1997, *A&AR*, 8, 1
Michaud G., Richard O., Richer J., VandenBerg D. A., 2004, *ApJ*, 606, 452
Montgomery K. A., Marschall L. A., Janes K. A., 1993, *AJ*, 106, 181
Nieuwenhuijzen H., de Jager C., 1990, *A&A*, 231, 134
Plummer H. C., 1911, *MNRAS*, 71, 460
Pols O. R., Schröder K.-P., Hurley J. R., Tout C. A., Eggleton P. P., 1998, *MNRAS*, 298, 525
Portegies Zwart S. F., Hut P., Makino J., McMillan S. L. W., 1998, *A&A*, 337, 363
Portegies Zwart S. F., McMillan S. L. W., Hut P., Makino J., 2001, *MNRAS*, 321, 199
Portegies Zwart S. F., Makino J., McMillan S. L. W., Hut P., 2002, *ApJ*, 565, 265
Reimers D., 1975, *Mem. Soc. R. Sci. Liege*, 8, 369

- Salaris M., Weiss A., Percival S. M., 2004, *A&A*, 414, 163
Salpeter E. E., 1955, *ApJ*, 121, 161
Schaller G., Schaerer D., Meynet G., Maeder A., 1992, *A&AS*, 96, 269
Smith H., 1977, *A&A*, 61, 305
Terlevich E., 1987, *MNRAS*, 224, 193
VandenBerg D. A., Swenson F. J., Rogers F. J., Iglesias C. A., Alexander D. R., 2000, *ApJ*, 532, 430
Vesperini E., HEGGIE D. C., 1997, *MNRAS*, 289, 898
Vesperini E., Zepf S. E., 2003, *ApJ*, 587, L97
Vine S. G., Bonnell I. A., 2003, *MNRAS*, 342, 314
Wilkinson M. I., Hurley J. R., Mackey A. D., Gilmore G. F., Tout C. A., 2003, *MNRAS*, 343, 1025
Yi S. K., Kim Y.-C., Demarque P., 2003, *ApJS*, 144, 259

This paper has been typeset from a $\text{\TeX}/\text{\LaTeX}$ file prepared by the author.